Heterodimer Formation between Superoxide Dismutase and Its Copper Chaperone †

ARTICLE *in* BIOCHEMISTRY · JANUARY 2001

Impact Factor: 3.02 · DOI: 10.1021/bi002207a · Source: PubMed

Accelerated Publications

Heterodimer Formation between Superoxide Dismutase and Its Copper Chaperone†

Audrey L. Lamb,‡ Andrew S. Torres,§ Thomas V. O'Halloran,‡,§ and Amy C. Rosenzweig*,‡,§

Department of Biochemistry, Molecular Biology, and Cell Biology and Department of Chemistry, Northwestern University, Evanston, Illinois 60208

Received September 19, 2000; Revised Manuscript Received October 16, 2000

ABSTRACT: Copper, zinc superoxide dismutase (SOD1) is activated in vivo by the copper chaperone for superoxide dismutase (CCS). The molecular mechanisms by which CCS recognizes and docks with SOD1 for metal ion insertion are not well understood. Two models for the oligomerization state during copper transfer have been proposed: a heterodimer comprising one monomer of CCS and one monomer of SOD1 and a dimer of dimers involving interactions between the two homodimers. We have investigated protein−protein complex formation between copper-loaded and apo yeast CCS (yCCS) and yeast SOD1 for both wild-type SOD1 (wtSOD1) and a mutant SOD1 in which copper ligand His 48 has been replaced with phenylalanine (H48F-SOD1). According to gel filtration chromatography, dynamic light scattering, analytical ultracentrifugation, and chemical cross-linking experiments, yCCS and this mutant SOD1 form a complex with the correct molecular mass for a heterodimer. No higher order oligomers were detected. Heterodimer formation is facilitated by the presence of zinc but does not depend on copper loading of yCCS. The complex formed with H48F-SOD1 is more stable than that formed with wtSOD1, suggesting that the latter is a more transient species. Notably, heterodimer formation between copper-loaded yCCS and wtSOD1 is accompanied by SOD1 activation only in the presence of zinc. These findings, taken together with structural, biochemical, and genetic studies, strongly suggest that in vivo copper loading of yeast SOD1 occurs via a heterodimeric intermediate.

Copper, zinc superoxide dismutase (SOD1)[1] protects cells against oxidative damage by catalyzing the conversion of superoxide to dioxygen and hydrogen peroxide (*1*). SOD1, which is found in the cytoplasm of eukaryotic cells, is a 32 kDa homodimer. Each 16 kDa monomer houses a dinuclear copper- and zinc-containing active site where superoxide is disproportionated by a redox cycling of the copper ion. The Cu(II) form of the enzyme is reduced by superoxide to produce dioxygen and the reduced Cu(I) enzyme oxidized by another superoxide molecule to yield hydrogen peroxide (*2*, *3*). SOD1 is activated in vivo by the *c*opper *c*haperone for *s*uperoxide dismutase (CCS) (*4*, *5*), which belongs to an emerging family of metal trafficking proteins called metallochaperones (*6*, *7*). These proteins deliver copper ions to specific target proteins by direct protein−protein interactions. Initially discovered in yeast (yCCS) (*4*), CCS homologues have also been identified in humans (hCCS) (*4*), mice (*8*), and plants (*9*).

The recent crystal structure of full-length yCCS revealed a dimer (54 kDa), each monomer (27 kDa) in which comprises two domains (*10*). The N-terminal domain (domain I) exhibits a $\beta\alpha\beta\beta\alpha\beta$ fold similar to that of the copper chaperone Atx1 (*11*) and its structural homologues (*6*). Like Atx1, this domain contains a MT/HCXXC metal binding motif (*12*). The second domain (domain II) resembles SOD1 in overall fold but lacks two key loop structures that generate the SOD1 active site (*2*, *13*, *14*). The first, the zinc subloop, provides the ligands to the zinc ion. The second, the electrostatic channel loop, forms a channel that guides superoxide to the catalytic center by charge differential (*15*). These loops are present in hCCS domain II, which has also been crystallographically characterized (*16*), but neither yCCS nor hCCS contains a copper binding site in this domain. Two additional loops, corresponding to the SOD1 S−S subloop and Greek key loop (*17*, *18*), are structurally conserved in both yCCS and hCCS. These two loops form

† This work was supported by NIH Grants GM58518 (to A.C.R.) and GM5411 (to T.V.O.), by grants from the ALS Association (to A.C.R. and to T.V.O.), by NIH NRSA Fellowship GM19973 (to A.L.L.), and by the Illinois Minority Graduate Incentive Program (to A.S.T.).

* Address correspondence to this author. Telephone: (847) 467-5301. Fax: (847) 467-6489. E-mail: amyr@northwestern.edu.

‡ Department of Biochemistry, Molecular Biology, and Cell Biology.

§ Department of Chemistry.

[1] Abbreviations: SOD1, copper, zinc superoxide dismutase; CCS, copper chaperone for superoxide dismutase; yCCS, yeast copper chaperone for superoxide dismutase; hCCS, human copper chaperone for superoxide dismutase; MES, 2-(*N*-morpholino)ethanesulfonic acid; EDTA, ethylenediaminetetraacetic acid; DTT, dithiothreitol; ICP-AES, inductively coupled plasma atomic emission spectroscopy; wtSOD1, wild-type yeast SOD1; H48F-SOD1, H48F mutant of yeast SOD1; Cu-yCCS, copper loaded form of yCCS; BCS, bathocuproinedisulfonic acid; MALDI-TOF, matrix-assisted laser desorption/ionization time of flight; EDC, 1-ethyl-3-(3-dimethylaminopropyl)carbodiimide hydrochloride; SOD, superoxide dismutase; NBT, nitroblue tetrazolium; FALS, familial amyotrophic lateral sclerosis.

10.1021/bi002207a CCC: $19.00
Published on Web 11/10/2000

a large part of the dimer interface in both SOD1 and CCS. A C-terminal domain (domain III) that contains a CXC potential metal binding motif (*19*) is disordered in the yCCS structure. The structural data combined with truncation mutagenesis studies in yeast (*19*) suggest that domain I and domain III function in metal uptake and delivery whereas domain II plays a role in target recognition.

The molecular mechanisms by which domain II recognizes and docks with SOD1 for copper delivery have not been elucidated, but comparisons of the chaperone and target enzyme crystal structures have led to two models. First, metal insertion into SOD1 by CCS could be accomplished by the formation of a heterodimer between the two proteins (*10*, *16*, *20*). In this model, one monomer of CCS exploits the conserved dimer interface to form a complex with one monomer of SOD1. Comparison of the yCCS and SOD1 structures indicates that heterodimer formation is feasible (*10*). Moreover, heterodimer formation between different SOD1s has been reported (*21*, *22*). Second, metal ion transfer from chaperone to SOD1 could occur by the formation of higher order oligomers such as a dimer of dimers (*10*, *16*, *20*, *23*). In support of this model, hCCS is dimeric in solution (*16*, *20*), yCCS is dimeric in the crystal (*10*) and in solution under some conditions (*19*, *23*), and the SOD1 homodimer is quite stable (*24*). To test these two models, we have investigated protein−protein complex formation between yCCS and yeast SOD1.

EXPERIMENTAL PROCEDURES

Protein Purification and Mutagenesis. The yCCS protein was expressed as described previously (*5*) and recovered from the cell pellet by freeze−thaw extraction. After centrifugation at 10000*g* for 20 min at 4 °C, the protein was loaded onto a Q Sepharose Fast Flow column (Pharmacia) equilibrated in 50 mM MES, pH 6.0, containing 1 mM EDTA and 20 mM DTT. Fractions containing yCCS eluted in the wash and were dialyzed against 50 mM MES, pH 6.0, with 1 mM EDTA and 20 mM DTT overnight. The sample was then applied to a SP Sepharose Fast Flow column (Pharmacia) equilibrated in the same buffer as the Q Sepharose column, and yCCS was eluted with a 0−500 mM NaCl gradient. Fractions containing yCCS eluted at approximately 140 mM NaCl and were estimated to be greater than 99% pure by SDS−PAGE using Coomassie stain. The purified yCCS contained no copper or zinc as determined by inductively coupled plasma atomic emission spectroscopy (ICP-AES). The protein concentration was determined using a calibrated Bradford assay with IgG as the protein standard (*5*).

The pET3d expression vector for yeast wild-type SOD1 (wtSOD1) was used to generate the H48F mutant (H48F-SOD1) as described elsewhere (*25*). The following procedure was used to purify both the wild-type and mutant proteins. Transformed *Escherichia coli* strain BL21(DE3) was grown in Luria broth to an optical density at 600 nm of 0.6−0.8, and SOD1 expression was induced with 1.0 mM IPTG. After 3 h, the cells were harvested and lysed by freeze−thaw extraction. All buffers used in the subsequent purification steps contained 1 mM EDTA and 20 mM DTT. The cell lysate was centrifuged at 10000*g* for 20 min at 4 °C, and the supernatant was dialyzed against 2.5 mM potassium phosphate, pH 7.8, overnight. The sample was then applied to a Q Sepharose Fast Flow column (Pharmacia), and SOD1 was eluted using a gradient of 2.5 mM potassium phosphate, pH 7.8, to 200 mM potassium phosphate, pH 7.8, with 500 mM NaCl. Fractions containing SOD1 eluted at approximately 50 mM potassium phosphate, pH 7.8, and 125 mM NaCl and were dialyzed against 50 mM MES, pH 6.0, overnight. The dialysate was loaded onto a SP Sepharose Fast Flow column (Pharmacia) equilibrated in 50 mM MES, pH 6.0, and SOD1 was eluted with a 0−500 mM NaCl gradient. Fractions containing SOD1 eluted at approximately 425 mM NaCl. The purified material was estimated to be greater than 99% pure by SDS−PAGE with Coomassie stain and contained no copper or zinc according to metal analysis by ICP-AES. Protein concentrations for both wt- and H48F-SOD1 were calculated using $\epsilon_{278} = 3230\ M^{-1}\ cm^{-1}$ per dimer (*26*).

Preparation of Cu-yCCS. The copper-loaded form of yCCS (Cu-yCCS) was prepared as previously described (*5*) with some modifications. Purified yCCS (100 μM) in 50 mM MES/Tris, pH 8.0, containing 10 mM DTT, 10 mM glutathione, 10 mM histidine, and 200 mM NaCl was incubated with 2 molar equiv of $Cu^{I}(CH_3CN)_4PF_6$ overnight at room temperature. Excess Cu(I) was removed by five cycles of dilution and concentration in the same buffer using an Amicon stirred cell. Finally, the protein was exchanged into 100 mM MES, pH 6.0, using a PD-10 desalting column (Pharmacia). All stages of the metalation procedure were carried out in a Coy anaerobic chamber. The final sample contained ~1.5 copper ions per monomer as determined by ICP-AES and the Bradford assay calibrated for yCCS (*5*).

Protein−Protein Complex Formation. For complex formation, yCCS, Cu-yCCS, H48F-SOD1, and wtSOD1 were exchanged into 100 mM MES, pH 6.0, treated with Chelex 100 resin (Bio-Rad) using PD-10 desalting columns (Pharmacia). Eight different reaction mixtures were tested for complex formation (Table 1). The protein concentrations (per monomer) were 40 μM for yCCS and Cu-yCCS and 80 μM for H48F-SOD1 and wtSOD1. In reaction mixtures 2, 4, 6, and 8, $ZnSO_4$ was added to a final concentration of 100 μM. Bathocuproinedisulfonic acid (BCS) was added to a final concentration of 100 μM in reaction mixtures 5, 6, 7, and 8 to prevent nonspecific loading of copper into SOD1 from solution (*5*). Reactions 1−4 were conducted in air whereas reactions 5−8 were conducted in the anaerobic chamber. All reaction mixtures were incubated at room temperature overnight.

Gel Filtration Chromatography. Gel filtration analysis of the reaction mixtures was performed using a Superdex 75 column (Pharmacia). For reaction mixtures 1, 3, 5, and 7, the column was equilibrated with 100 mM MES, pH 6.0, containing 150 mM NaCl and 20 mM DTT pretreated with Chelex-100 resin. The same buffer supplemented with 20 μM $ZnSO_4$ was used for reaction mixtures 2, 4, 6, and 8. This buffer was treated with Chelex-100 resin just prior to the addition of $ZnSO_4$. The Low Molecular Weight gel filtration calibration kit (Pharmacia) was used to estimate the molecular mass of proteins eluting from the Superdex 75 column. The peak for each reaction mixture that eluted between 58 and 68 mL (Figure 1, labeled P1, P2, P5, and P6, and comparable peaks for reactions 3, 4, 7, and 8) was collected and used for subsequent biophysical characterization and chemical cross-linking experiments. According to

SDS−PAGE analysis, each of these peaks contained both proteins. Matrix-assisted laser desorption/ionization time-of-flight (MALDI-TOF) mass spectrometric analysis of reaction mixture 2 revealed two polypeptides with molecular masses of 27 163 and 15 735 Da. These values agree well with the observed mass of yCCS (27 169 Da) (*5*) and the calculated mass of H48F-SOD1 (15 732.5 Da). The absence of higher molecular mass species indicates that the two proteins were not covalently linked by a disulfide bond.

Dynamic Light Scattering. Dynamic light scattering data were collected using a Brookhaven Instruments BI-9000AT autocorrelator, a BI-300SM goniometer, and a Lexel Laser Inc. Model 95 argon ion laser. The laser was operated at 514.5 nm at a power of 300 mW. Measurements were conducted at 22 °C. Samples were concentrated using Microcon YM-10 concentrators to ∼1−2 mg/mL, as determined by the calibrated Bradford assay for yCCS, ϵ_{278} for SOD1, and the standard Bradford assay for the reaction mixtures. Prior to measurement, samples were centrifuged using an airfuge at 30 psi to remove particulate matter. Size distribution analysis of autocorrelation functions was performed using the program CONTIN (*27, 28*).

Analytical Ultracentrifugation. Sedimentation equilibrium experiments were carried out using a Beckman XL-A analytical ultracentrifuge equipped with UV absorbance optics. Initial sample concentrations were chosen such that the absorbance at 280 nm was ∼0.25. All experiments were conducted at 10 °C using 120 μL samples and a four-hole AN-60 rotor spinning at 18 000 and 22 000 rpm. The absorbance was measured at 280 nm, and sedimentation equilibrium data were analyzed using the nonlinear regression program WinNonlin (*29*). For each sample, the absorbance at 280 nm versus radius data for two different velocities were analyzed simultaneously and fitted directly with a single ideal species model. The errors in Table 1 are an indication of the 95% confidence level of the global analysis as calculated by WinNonlin. The sigma values from WinNonlin were converted to molecular masses using the program SEDNTERP (*30*).

Chemical Cross-Linking. Samples were concentrated to ∼1−2 mg/mL, as determined by the Bradford assay, using Microcon YM-10 concentrators. The cross-linking agent 1-ethyl-3-(3-dimethylaminopropyl)carbodiimide hydrochloride (EDC) was added to a final concentration of 10 mg/mL, and the samples were incubated at room temperature for 2 h. Parallel reactions without EDC were incubated for 2 h as well. The cross-linking reactions were stopped by the addition of SDS−PAGE sample loading buffer (6% SDS, 15% 2-mercaptoethanol, 20% glycerol, 0.6% bromophenol blue), and the samples were analyzed by SDS−PAGE with Coomassie stain (*31*). For Western analysis, reaction mixture 2 with and without EDC treatment was separated on a 12% Tris SDS−PAGE gel, transferred to a Immuno-Blot PVDF membrane (Bio-Rad), and probed with highly specific polyclonal rabbit antibodies against CCS (*25*) at 1:5000 dilution or SOD1 at 1:5000 dilution followed by goat anti-rabbit IgG HRP conjugate at 1:8000 dilution (Bio-Rad). The proteins were detected with enhanced chemiluminescence reagents (Pharmacia).

Superoxide Dismutase Activity Assay. Superoxide dismutase (SOD) activity staining of native PAGE gels with nitroblue tetrazolium (NBT) was carried out as described previously (*32*). Native PAGE running buffer and sample loading buffer were treated with Chelex-100 resin prior to use. To ensure the presence of SOD1 in the samples used for the activity assay, the reaction mixtures were not separated by gel filtration chromatography. Instead, the reactions were loaded directly onto the native gel for the activity assay. SOD activity from nonspecific loading of copper into SOD1 or from free copper in solution was prevented by the addition of BCS to all eight reactions to a final concentration of 100 μM (*5*).

RESULTS

Complex Formation and Purification. A CCS/SOD1 complex is likely to be a transient species to facilitate copper transfer and not hinder catalytic function of SOD1. To trap the metal delivery complex, a mutant of yeast SOD1 that is incapable of binding copper was generated by site-directed mutagenesis. The copper ion in SOD1 is coordinated by four histidine residues. One of these histidines, His 63, also coordinates the zinc ion, bridging the dinuclear cluster (*13, 14, 18*). Since zinc binding could be important for copper delivery by yCCS, this bridging histidine was not selected for mutagenesis. Instead, copper ligand His 48 was replaced with phenylalanine. Phenylalanine was chosen because it is not likely to coordinate copper and because it would fill the cavity vacated by the histidine.

Both the H48F mutant and wtSOD1 were used for complex formation experiments with yCCS and Cu-yCCS

Table 1: Analysis of yCCS/SOD1 Complex Formation

Molecular Mass (kDa) of Key Species					
species	mol mass	species	mol mass	species	mol mass
SOD1 monomer	16	yCCS monomer	27	yCCS/SOD1 heterodimer	43
SOD1 dimer	32	yCCS dimer	54	yCCS/SOD1 dimer of dimers	86

Summary of Experimental Data				
reaction mixture	light scattering	analytical ultracentrifugation (kDa)	chemical cross-linking	SOD activity
(1) yCCS + H48F-SOD1	polydisperse	ND	+	−
(2) yCCS + H48F-SOD1 + Zn	monodisperse	42.0 ± 3.5	+++	−
(3) yCCS + wtSOD1	polydisperse	ND	+	−
(4) yCCS + wtSOD1 + Zn	monodisperse	33.7 ± 3.3	++	−
(5) Cu-yCCS + H48F-SOD1	ND	ND	++	−
(6) Cu-yCCS + H48F-SOD1 + Zn	monodisperse	38.1 ± 2.2	+++	−
(7) Cu-yCCS + wtSOD1	polydisperse	ND	++	−
(8) Cu-yCCS + wtSOD1 + Zn	monodisperse	32.3 ± 3.1	++	+

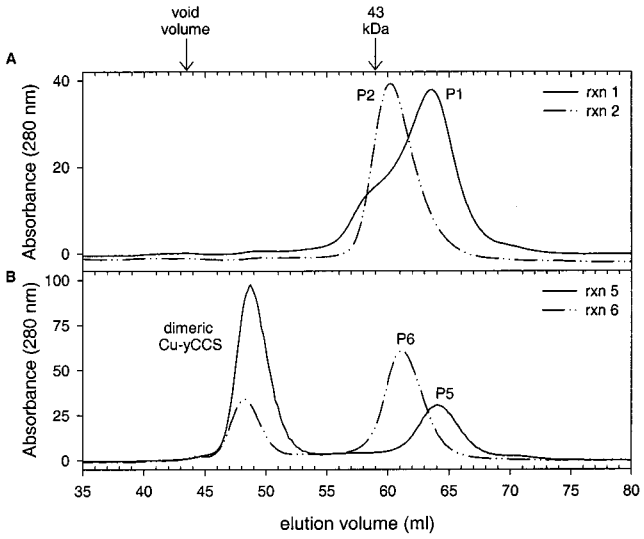

FIGURE 1: Gel filtration chromatographic analysis of yCCS/H48F-SOD1 complex formation. (A) Representative traces for reaction mixtures with apo yCCS. Peaks P1 (reaction mixture 1, yCCS/H48F-SOD1) and P2 (reaction mixture 2, yCCS/H48F-SOD1/Zn) contained both yCCS and SOD1. The addition of 100 μM $ZnSO_4$ promotes a shift in elution volume, suggestive of yCCS/SOD1 complex formation. (B) Representative traces for reaction mixtures with Cu-yCCS. Peaks P5 (reaction mixture 5, Cu-yCCS/H48F-SOD1) and P6 (reaction mixture 6, Cu-yCCS/H48F-SOD1/Zn) contained both yCCS and SOD1. Zinc promotes a shift in elution volume and a decrease in the amount of dimeric Cu-yCCS.

in the absence and presence of zinc (Table 1). After incubation overnight, each of the mixtures was analyzed by gel filtration chromatography using a Superdex 75 column. Figure 1 shows four representative gel filtration traces. Since SOD1 has a low extinction coefficient at 280 nm (*26*), the detected peaks primarily represent yCCS. The individual peaks were collected, and SDS−PAGE analysis in combination with the observed elution volume from the gel filtration column revealed that the peak eluting between 46 and 51 mL (Figure 1B) is dimeric Cu-yCCS. Dimerization of Cu-yCCS has been observed previously (*19*). In the absence of DTT, dimeric apo yCCS was also detected (data not shown). The other peaks (P1, P2, P5, P6) all contained both yCCS (27 kDa monomer) and SOD1 (32 kDa dimer) and eluted at volumes consistent with a molecular mass of ~30−40 kDa. These peaks could therefore correspond to monomeric Cu-yCCS and dimeric SOD1 eluting simultaneously, to a complex of monomeric yCCS and monomeric SOD1 or to a mixture of these species. The analogous experiments with wtSOD1 (reaction mixtures 3, 4, 7, and 8) gave comparable traces (data not shown). In the presence of zinc, the peak containing both yCCS and SOD1 eluted earlier, indicating the formation of a higher molecular mass species (P2, P6). This species was detected with both apo and Cu-yCCS. For Cu-yCCS, the shift in elution volume was accompanied by a significant decrease in the amount of dimeric Cu-yCCS.

One explanation for the shift in elution volume upon zinc addition is that the new peak represents a yCCS/SOD1 complex (P2, P6) whereas the peak observed in the absence of zinc (P1, P5) contains both monomeric CCS and dimeric SOD1. This interpretation suggests that zinc plays a role in complex formation. For Cu-yCCS, zinc addition is accompanied by the disappearance of dimeric Cu-yCCS and the appearance of an ~40 kDa complex (Figure 1B). Although the same shift occurs for apo yCCS, the gel filtration trace indicates that some of the putative complex is present in the absence of zinc (Figure 1A, P1). The gel filtration data are not conclusive evidence for yCCS/SOD1 complex formation, however. The elution profiles of yCCS or Cu-yCCS individually vary considerably with protein, reductant, and salt concentrations. In addition, the very low ϵ_{280} for SOD1 prevented detection of SOD1 as it eluted from the gel filtration column except at very high concentrations. To determine whether a complex was indeed forming and to establish its oligomerization state, the peaks eluting between 58 and 68 mL (P1, P2, P5, P6, and comparable peaks for reactions 3, 4, 7, and 8) were collected and used for subsequent biophysical characterization.

Dynamic Light Scattering. Samples separated by gel filtration chromatography and pure samples of yCCS, wt-SOD1, and H48F−SOD1 in the absence and presence of zinc were used to obtain dynamic light scattering autocorrelation functions. For SOD1 and yCCS without zinc, size distribution analysis revealed a considerable amount of polydispersity, indicating the presence of aggregated species (Figure 2A). Although SOD1 remains polydisperse upon zinc addition, yCCS becomes more monodisperse (Figure 2B). Samples from the gel filtration column containing both yCCS and SOD1 are polydisperse, but the predominant species has a Stokes diameter of 5 nm (Figure 2C). The inclusion of zinc in the reaction mixtures yielded the most striking result. These samples are monodisperse and contain a species with a Stokes diameter of approximately 5 nm (Figure 2D, Table 1).

Analytical Ultracentrifugation. To investigate the association behavior of the potential yCCS/SOD1 complex, analytical ultracentrifugation sedimentation equilibrium experiments were conducted on samples that were monodisperse by light scattering. Two representative nonlinear regression fits of the concentration distribution are shown in Figure 3. The concentration distribution was fitted well with a single ideal species model, and the resultant values of the molecular mass for each reaction mixture are listed in Table 1. Only the reaction mixtures with zinc and H48F-SOD1 (reactions 2 and 6) contain a species larger than the individual proteins. The molecular mass of 42 kDa for yCCS/H48F-SOD1/Zn is consistent with the calculated molecular mass of a heterodimeric complex (~43 kDa). The molecular mass of 38 kDa for Cu-yCCS/H48F-SOD1/Zn (reaction 6) may indicate that this reaction mixture contains small amounts of monomeric yCCS (27 kDa) and dimeric SOD1 (32 kDa) in addition to the heterodimer. The values obtained for the wtSOD1 reaction mixtures are closer to 30 kDa and indicate that monomeric yCCS and dimeric SOD1 are the main species present.

Chemical Cross-Linking. The results of covalent cross-linking of yCCS and SOD1 with EDC are shown in Figure 4 and Table 1. Both wtSOD1 and H48F-SOD1 consistently migrate more slowly than comparable molecular mass standards. Cross-linking of the eight reaction mixtures resulted in the formation of a new ~43 kDa band, which indicates a linkage between a monomer of yCCS and a monomer of SOD1. Western blot analysis confirms that this band contains both proteins (Figure 4C). In contrast to the analytical ultracentrifugation data, this heterodimeric complex is observed for wtSOD1 as well as for H48F-SOD1.

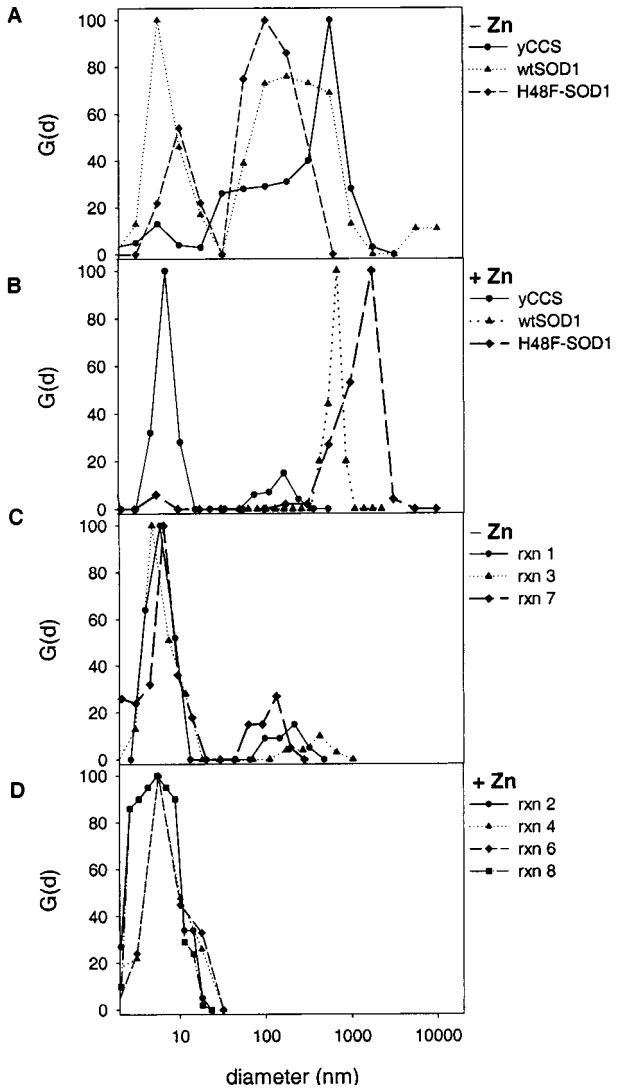

FIGURE 2: CONTIN size distribution analysis of dynamic light scattering autocorrelation functions. $G(d)$ is the intensity-weighted distribution of scatterers having Stokes diameter = d. (A) $G(d)$ versus Stokes diameter for yCCS, wtSOD1, and H48F-SOD1. (B) $G(d)$ versus Stokes diameter for yCCS, wtSOD1, and H48F-SOD1 in the presence of 100 μM $ZnSO_4$. (C) $G(d)$ versus Stokes diameter for reaction mixture 1 (yCCS/H48F-SOD1), reaction mixture 3 (yCCS/wtSOD1), and reaction mixture 7 (Cu-yCCS/wtSOD1). (D)-$G(d)$ versus Stokes diameter for reaction mixture 2 (yCCS/H48F-SOD1/Zn), reaction mixture 4 (yCCS/wtSOD1/Zn), reaction mixture 6 (Cu-yCCS/H48F-SOD1/Zn), and reaction mixture 8 (Cu-yCCS/wtSOD1/Zn).

Although all eight reaction mixtures contain cross-linked heterodimer, the intensity of the heterodimeric band varies. This effect is most pronounced in the reactions with H48F-SOD1. For these reactions, more intense heterodimeric bands are observed upon zinc addition (Figure 4A, reaction mixture 2, and Figure 4B, reaction mixture 6). If the intensity of this band correlates with complex stability, the most stable heterodimeric species is formed between H48F-SOD1 and yCCS in the presence of zinc. Although zinc is not strictly required, it clearly facilitates complex formation.

SOD Activity. All eight reaction mixtures were tested for SOD activity by NBT staining on native gels (Figure 4D and Table 1). The resulting SOD activity bands show that wtSOD1 is only activated when both Cu-yCCS and zinc are present (reaction 8). H48F-SOD1 does not exhibit SOD activity under any conditions, and wtSOD1 is not activated in the absence of zinc or without copper-loaded chaperone.

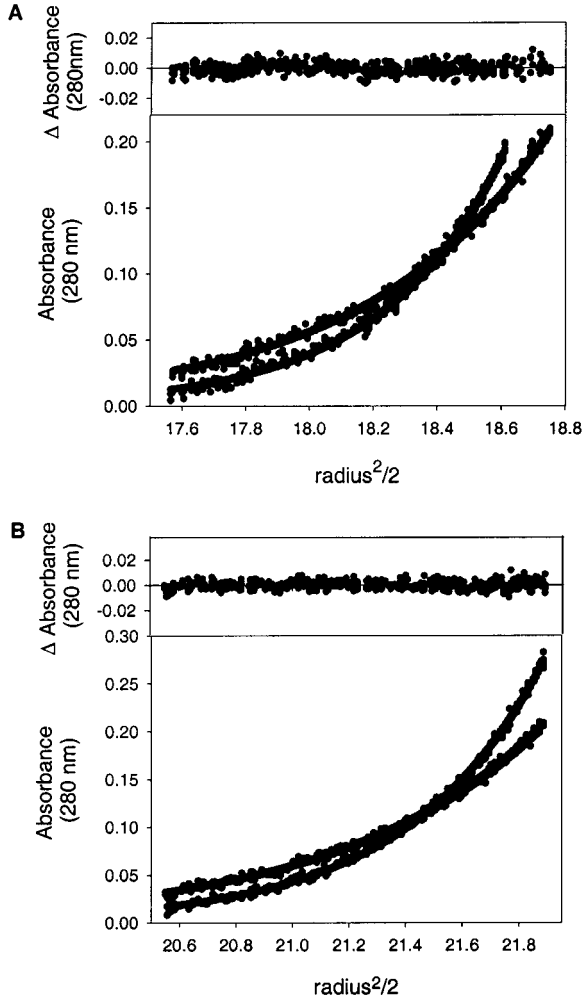

FIGURE 3: Sedimentation equilibrium analysis of complex formation. Samples were centrifuged at two speeds (18 000 and 22 000 rpm) as described in Experimental Procedures. The data from two representative samples are shown. The lower panel shows the fits to the raw data from 10 absorbance scans taken at 280 nm as a function of radial position and the corresponding fitted curve, and the upper panel shows the distribution of residuals. The data were fit to the single ideal species model. (A) Reaction mixture 2 (yCCS/H48F-SOD1/Zn). (B) Reaction mixture 4 (yCCS/wtSOD1/Zn).

DISCUSSION

The results presented here provide strong evidence for the formation of a specific protein−protein complex between yCCS and SOD1. The dynamic light scattering data show that the individual proteins are polydisperse but are converted to a monodisperse sample upon mixing. This observation indicates that the two proteins are interacting. The molecular mass of the protein−protein complex determined from the analytical ultracentrifugation and chemical cross-linking data, ~43 kDa, is most consistent with a heterodimer comprising one monomer of yCCS (27 kDa) and one monomer of SOD1 (16 kDa). The gel filtration data are also compatible with heterodimer formation. Higher order complexes, such as a dimer of dimers (*10*, *16*, *23*), were not detected. On the basis of the crystal structures (*10*, *14*), the heterodimer probably involves conserved residues located at the homodimer interfaces in yCCS domain II and SOD1. This conclusion is

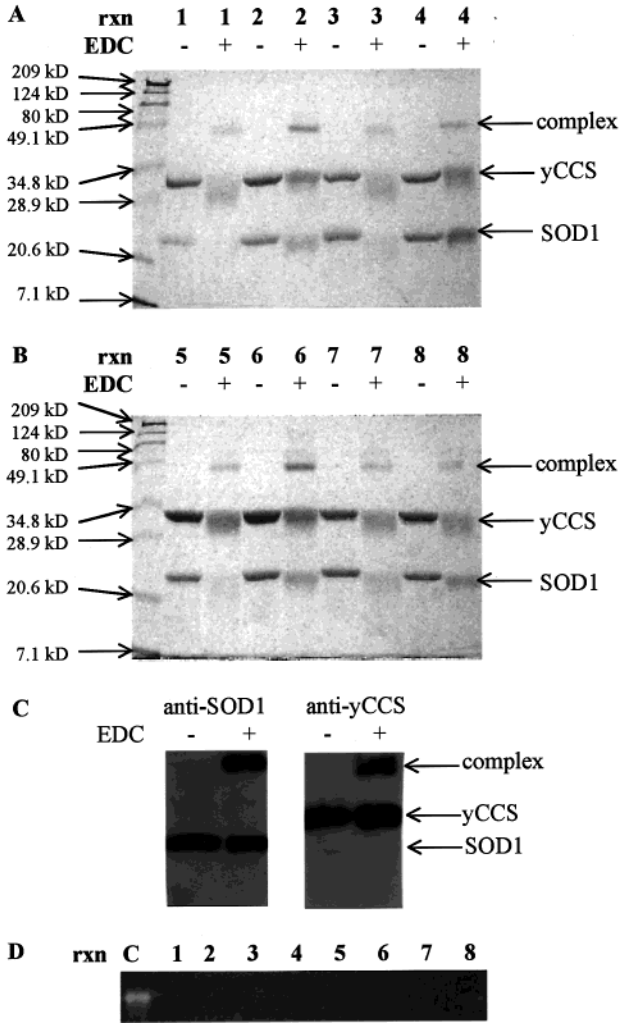

FIGURE 4: Chemical cross-linking and SOD activity data. (A) SDS−PAGE analysis of the cross-linking experiment in the absence of copper. Lane 1 contains the protein molecular mass standards. Lanes 2, 4, 6, and 8 correspond to non-cross-linked reaction mixtures 1 (yCCS/H48F-SOD1), 2 (yCCS/H48F-SOD1/Zn), 3 (yCCS/wtSOD1), and 4 (yCCS/wtSOD1/Zn), respectively. Lanes 3, 5, 7, and 9 correspond to cross-linked reaction mixtures 1, 2, 3, and 4. (B) SDS−PAGE of the cross-linking experiment in the presence of copper. Lane 1 contains the protein molecular mass standards. Lanes 2, 4, 6, and 8 correspond to non-cross-linked reaction mixtures 5 (Cu-yCCS/H48F-SOD1), 6 (Cu-yCCS/H48F-SOD1/Zn), 7 (Cu-yCCS/wtSOD1), and 8 (Cu-yCCS/wtSOD1/Zn). Lanes 3, 5, 7, and 9 correspond to cross-linked reaction mixtures 5, 6, 7, and 8, respectively. (C) Western blot analysis of reaction mixture 2 using an anti-SOD1 polyclonal antibody (left) and an anti-yCCS polyclonal antibody (right). (D) Native PAGE of the complexation reactions stained with NBT, riboflavin, and TEMED for SOD activity. Lane 1 contains human SOD purchased from Sigma (positive control). Lanes 2−9 correspond to reaction mixtures 1−8.

supported by recent observations that mutations at the dimer interfaces of either CCS or SOD1 prevent interaction of the two proteins and SOD1 activation in yeast cells (*33*). Although the SOD1 dimer is very stable (*24*), heterodimer formation between different SOD1 isozymes (*21*) and SOD1s from different organisms (*22*) has been observed. Furthermore, other tightly associated homodimers readily exchange to form heterodimers (*34*). These precedents, combined with the data presented here, indicate that the stability of the SOD1 dimer does not preclude copper loading via a heterodimeric intermediate.

All of the experimental data indicate that heterodimer formation is facilitated by the presence of zinc. In the gel filtration analysis, zinc promotes a shift in elution volume of the peak containing both yCCS and SOD1. The addition of zinc also results in the formation of a more homogeneous sample as determined by light scattering and the formation of a stable complex detectable by analytical ultracentrifugation. Moreover, a greater amount of cross-linked complex is observed in the presence of zinc. Not only does heterodimer form more readily with zinc but yCCS can only activate SOD1 in the presence of zinc. Since yCCS domain II does not contain a zinc binding site (*10*), the role of zinc may be related to the SOD1 zinc site. Zinc binding is known to cause conformational changes in the loop regions of SOD1 (*24*) and likely stabilizes both the zinc subloop and the S−S subloop, which is N-terminal to the zinc subloop and part of the same loop structure (*14*). The S−S subloop is involved in the SOD1 dimer interface (*14*) as is the equivalent loop in yCCS (*10*). The affinity of the two SOD1 monomers for one another is influenced by both the occupancy of the metal sites and the integrity of the disulfide bond between the S−S subloop and the β barrel structure (*24*). By analogy, the affinity of SOD1 for yCCS might depend on conformational priming of the SOD1 dimer interface region by zinc binding. According to this hypothesis, once zinc is bound to SOD1, the two proteins can form a heterodimer using the conserved dimer interfaces. Copper transfer via this heterodimeric complex would explain why SOD1 activation requires the presence of zinc. It is also possible that yCCS assists in zinc loading of SOD1 either directly or as a molecular chaperone.

Although complex formation is facilitated by zinc, it is apparently independent of whether copper is bound to yCCS. A Cu-yCCS homodimer is detected in the gel filtration trace, and the elution volume of the peaks containing both yCCS and SOD1 is only slightly altered by copper (Figure 1). This shift may be due to a conformational change in yCCS upon copper binding. In addition, a comparison of the light scattering, analytical ultracentrifugation, and cross-linking data for the reaction mixtures reveals only subtle differences upon copper loading of yCCS. These observations are not surprising for two reasons. First, binding of copper to CCS need not be a prerequisite for docking with SOD1 in vivo (*33*, *35*). Second, the two metal binding motifs in yCCS are located in domain I (MT/HCXXC) and domain III (CXC). A structure of copper-loaded CCS is not available, but recent biochemical (*19*, *20*) and spectroscopic (*9*, *36*) data suggest that the four cysteines from domains I and III can participate in copper binding. If the heterodimer forms using conserved residues in domain II, copper binding at a site involving domains I and III may not necessarily affect complex formation. Moreover, although domain III is essential for interaction with SOD1, the two conserved cysteine residues are not required (*33*). Under other conditions copper may stabilize the heterodimeric complex but is not required for its formation (*25*).

The yCCS/SOD1 heterodimer described here is likely to represent the physiological docked complex. Mutations at the dimer interfaces of either CCS or SOD1 preclude protein−protein interactions and SOD1 activation in vivo (*33*). These data alone cannot distinguish between heterodimer and dimer of dimer models. The biophysical data indicate that only heterodimers and no higher molecular mass

complexes form between yCCS and SOD1, however. Taken together, these findings strongly suggest that in vivo copper loading of yeast SOD1 occurs by a heterodimeric intermediate. In further support, heterodimer formation between CuyCCS and wtSOD1 in the presence of zinc is accompanied by the appearance of SOD1 activity (Figure 4). Finally, a comparison of the wtSOD1 and H48F-SOD1 biophysical data is consistent with physiological heterodimer formation. The interaction between CCS and SOD1 is expected to be transient since dissociation of CCS after copper transfer is necessary for SOD1 to reach its fully active homodimeric state. Although the effects of zinc and copper on heterodimer formation are similar for wtSOD1 and H48F-SOD1, the complex formed between yCCS and H48F-SOD1 is apparently more stable. The yCCS/wtSOD1 heterodimer is evident in the cross-linking data but is not detectable in the analytical ultracentrifugation experiment, suggesting that it is a more transient species.

It is not yet clear how copper transfer is accomplished within the heterodimeric complex. Models of the heterodimer generated using the yCCS structure show that the metal binding motif in yCCS domain I is ~40 Å from the SOD1 active site (*6*, *23*), an obstacle that might be overcome by conformational changes in domains I and III. A detailed understanding of the copper transfer mechanism will require further characterization of the copper-loaded form of CCS and of the heterodimer. Knowledge of the heterodimer-mediated metal transfer mechanism is also potentially relevant to cases of familial amyotrophic lateral sclerosis (FALS) caused by mutations in human SOD1 (*37*, *38*). More than 70 mutations in SOD1 are linked to this progressively paralytic, fatal disease. A number of FALS mutations occur at the SOD1 dimer interface (*39*) and could prevent proper interaction with CCS. In addition, some FALS-related SOD1 mutants have a lower affinity for zinc (*40*, *41*), which could affect heterodimer formation and activation by CCS. Thus, structural and biophysical investigations of heterodimer formation between these mutants and CCS might provide new insight into the causes and treatment of SOD1-related FALS.

ACKNOWLEDGMENT

We thank J. Widom, T. Rae, and S. Garman for valuable discussions and N. Khidekel for excellent technical assistance. Dynamic light scattering and analytical ultracentrifugation data were collected in the Keck Biophysics Facility at Northwestern University.

REFERENCES

1. McCord, J. M., and Fridovich, I. (1969) *J. Biol. Chem. 244*, 6049−6055.
2. Bertini, I., Mangani, S., and Viezzoli, M. S. (1997) *Adv. Inorg. Chem. 45*, 127−250.
3. Lyons, T. J., Gralla, E. B., and Valentine, J. S. (1999) *Met. Ions Biol. Syst. 36*, 125−177.
4. Culotta, V. C., Klomp, L. W. J., Strain, J., Casareno, R. L. B., Krems, B., and Gitlin, J. D. (1997) *J. Biol. Chem. 272*, 23469−23472.
5. Rae, T. D., Schmidt, P. J., Pufahl, R. A., Culotta, V. C., and O'Halloran, T. V. (1999) *Science 284*, 805−808.
6. Rosenzweig, A. C., and O'Halloran, T. V. (2000) *Curr. Opin. Chem. Biol. 4*, 140−147.
7. O'Halloran, T. V., and Culotta, V. C. (2000) *J. Biol. Chem. 275*, 25057−25060.
8. Wong, P. C., Waggoner, D., Subramaniam, J. R., Tessarollo, L., Bartnikas, T. B., Culotta, V. C., Price, D. L., Rothstein, J., and Gitlin, J. D. (2000) *Proc. Natl. Acad. Sci. U.S.A. 97*, 2886−2891.
9. Zhu, H., Shipp, E., Sanchez, R. J., Liba, A., Stine, J. E., Hart, P. J., Gralla, E. B., Nersissian, A. M., and Valentine, J. S. (2000) *Biochemistry 39*, 5413−5421.
10. Lamb, A. L., Wernimont, A. K., Pufahl, R. A., O'Halloran, T. V., and Rosenzweig, A. C. (1999) *Nat. Struct. Biol. 6*, 724−729.
11. Rosenzweig, A. C., Huffman, D. L., Hou, M. Y., Wernimont, A. K., Pufahl, R. A., and O'Halloran, T. V. (1999) *Structure 7*, 605−617.
12. Bull, P. C., and Cox, D. W. (1994) *Trends Genet. 10*, 246−252.
13. Tainer, J. A., Getzoff, E. D., Beem, K. M., Richardson, J. S., and Richardson, D. C. (1982) *J. Mol. Biol. 160*, 181−217.
14. Djinovic, K., Gatti, G., Coda, A., Antolini, L., Pelosi, G., Desideri, A., Falconi, M., Marmocchi, F., Rotilio, G., and Bolognesi, M. (1992) *J. Mol. Biol. 225*, 791−809.
15. Getzoff, E. D., Tainer, J. A., Weiner, P. K., Kollman, P. A., Richardson, J., and Richardson, D. C. (1983) *Nature 306*, 287−290.
16. Lamb, A. L., Wernimont, A. K., Pufahl, R. A., O'Halloran, T. V., and Rosenzweig, A. C. (2000) *Biochemistry 39*, 1589−1595.
17. Getzoff, E. D., Tainer, J. D., Stempien, M. M., Bell, G. I., and Hallewell, R. A. (1989) *Proteins 5*, 322−336.
18. Bordo, D., Djinovic, K., and Bolognesi, M. (1994) *J. Mol. Biol. 238*, 366−386.
19. Schmidt, P. J., Rae, T. D., Pufahl, R. A., Hamma, T., Strain, J., O'Halloran, T. V., and Culotta, V. C. (1999) *J. Biol. Chem. 274*, 23719−23725.
20. Rae, T. D., Torres, A. S., Pufahl, R. A., and O'Halloran, T. V. (2000) *J. Biol. Chem*. (in press).
21. Capo, C. R., Polticelli, F., Calabrese, L., Schinina, M. E., Carri, M. T., and Rotilio, G. (1990) *Biochem. Biophys. Res. Commun. 173*, 1186−1193.
22. Tegelström, H. (1975) *Hereditas 81*, 185−198.
23. Hall, L. T., Sanchez, R. J., Holloway, S. P., Zhu, H., Stine, J. E., Lyons, T. J., Demeler, B., Schirf, V., Hansen, J. C., Nersissian, A. M., Valentine, J. S., and Hart, P. J. (2000) *Biochemistry 39*, 3611−3623.
24. Valentine, J. S., and Pantoliano, M. W. (1981) in *Copper Proteins* (Spiro, T. G., Ed.) pp 291−358, Wiley-Interscience, New York.
25. Torres, A. S., Rae, T., and O'Halloran, T. V. (submitted for publication).
26. Lyons, T. J., Nerissian, A., Goto, J. J., Zhu, H., Gralla, E. B., and Valentine, J. S. (1998) *J. Biol. Inorg. Chem. 3*, 650−662.
27. Provencher, S. W. (1982) *Comput. Phys. Commun. 27*, 213−227.
28. Provencher, S. W. (1982) *Comput. Phys. Commun. 27*, 229−242.
29. Johnson, M. L., Correia, J. J., Yphantis, D. A., and Halvorson, H. R. (1981) *Biophys. J. 36*, 575−588.
30. Laue, T. M., Shah, B. D., Ridgeway, T. M., and Pelletier, S. L. (1992) in *Analytical Ultracentrifugation in Biochemistry and Polymer Science* (Harding, S., and Rowe, A., Eds.) pp 90−125, Royal Society of Chemistry, Cambridge.
31. Fox, B. G., Liu, Y., Dege, J. E., and Lipscomb, J. D. (1991) *J. Biol. Chem. 266*, 540−550.
32. Flohé, L., and Öetting, F. (1984) *Methods Enzymol. 105*, 93−104.
33. Schmidt, P. J., Kunst, C., and Culotta, V. C. (2000) *J. Biol. Chem. 275*, 33771−33776.
34. Hejtmancik, J. F., Wingfield, P. T., Chambers, C., Russell, P., Chen, H.-C., Sergeev, Y. V., and Hope, J. N. (1997) *Protein Eng. 10*, 1347−1352.
35. Casareno, R. L. B., Waggoner, D., and Gitlin, J. D. (1998) *J. Biol. Chem. 273*, 23625−23628.
36. Eisses, J. F., Stasser, J. P., Ralle, M., Kaplan, J. H., and Blackburn, N. J. (2000) *Biochemistry 39*, 7337−7342.

37. Deng, H.-X., Hentati, A., Tainer, J. A., Iqbal, Z., Cayabyab, A., Hung, W.-Y., Getzoff, E. D., Hu, P., Herzfeldt, B., Roos, R. P., Warner, C., Deng, G., Soriano, E., Smyth, C., Parge, H. E., Ahmed, A., Roses, A. D., Hallewell, R. A., Pericak-Vance, M. A., and Siddique, T. (1993) *Science 261*, 1047−1051.
38. Rosen, D. R., et al. (1993) *Nature 362*, 59−62.
39. Siddique, T., Nijhawan, D., and Hentati, A. (1997) *J. Neural Transm. 49*, 219−233.
40. Estévez, A. G., Crow, J. P., Sampson, J. B., Reiter, C., Zhuang, Y., Richardson, G. J., Tarpey, M. M., Barbeito, L., and Beckman, J. S. (1999) *Science 286*, 2498−2500.
41. Lyons, T. J., Nersissian, A., Huang, H., Yeom, H., Nishida, C. R., Graden, J. A., Gralla, E. B., and Valentine, J. S. (2000) *J. Biol. Inorg. Chem. 5*, 189−203.

BI002207A